

Another forbidden solar oxygen abundance: the [O I] 5577 Å line

J. Meléndez^{1,2} and M. Asplund³

¹ Centro de Astrofísica da Universidade do Porto, Rua das Estrelas, 4150-762 Porto, Portugal

² Research School of Astronomy & Astrophysics, Australian National University, Mt. Stromlo Observatory, Weston ACT 2611, Australia

³ Max Planck Institute for Astrophysics, Postfach 1317, 85741 Garching, Germany

Received ...; accepted ...

ABSTRACT

Context. Recent works with improved model atmospheres, line formation, atomic and molecular data, and detailed treatment of blends, have resulted in a significant downward revision of the solar oxygen abundance.

Aims. Considering the importance of the Sun as an astrophysical standard and the current conflict of standard solar models using the new solar abundances with helioseismological observations we have performed a new study of the solar oxygen abundance based on the forbidden [O I] line at 5577.34 Å, not previously considered.

Methods. High-resolution ($R > 500\,000$), high signal-to-noise ($S/N > 1000$) solar spectra of the [O I] 5577.34 Å line have been analyzed employing both three-dimensional (3D) and a variety of 1D (spatially and temporally averaged 3D, Holweger & Müller, MARCS and Kurucz models with and without convective overshooting) model atmospheres.

Results. The oxygen abundance obtained from the [O I] 5577.3 Å forbidden line is almost insensitive to the input model atmosphere and has a mean value of $\log \epsilon_{\text{O}} = 8.71 \pm 0.02$ (σ from using the different model atmospheres). The total error (0.07 dex) is dominated by uncertainties in the $\log gf$ value (0.03 dex), apparent line variation (0.04 dex) and uncertainties in the continuum and line positions (0.05 dex).

Conclusions. The here derived oxygen abundance is close to the 3D-based estimates from the two other [O I] lines at 6300 and 6363 Å, the permitted O I lines and vibrational and rotational OH transitions in the infrared. Our study thus supports a low solar oxygen abundance ($\log \epsilon_{\text{O}} \approx 8.7$), independent of the adopted model atmosphere.

Key words. Sun: abundances - Sun: photosphere - Line: identification - Molecular data

1. Introduction

In recent years a significant reduction in the solar oxygen abundance has been proposed from $\log \epsilon_{\text{O}} \equiv \log(N_{\text{O}}/N_{\text{H}}) + 12 = 8.93$ (Lambert 1978; Sauval et al. 1984; Grevesse et al. 1984; Anders & Grevesse 1989) down to $\log \epsilon_{\text{O}} \approx 8.7$ or even lower (Allende Prieto et al. 2001, 2004; Holweger 2001; Asplund et al. 2004; Meléndez 2004; Socas-Navarro & Norton 2007; Caffau et al. 2008; but see Ayres et al. 2006, Ayres 2008, and Centeno & Socas-Navarro 2008 for a departing conclusion). This large revision in the oxygen abundance has an important impact in many areas of astrophysics. In particular, solar models computed with the low oxygen abundance do not agree with precise helioseismological measurements (see Basu & Antia 2008 and references therein).

If the revised solar oxygen abundance is correct, this would imply that the standard solar structure model may be missing (or have a too simplified treatment of) important physical processes, which would carry over to errors in the calculations of stellar evolution at large. On the other hand, if the fault lies with the new solar photospheric abundance analyses it raises concerns about how well we understand stellar atmospheres and spectral line formation in general with wider implications for Galactic chemical evolution studies relying on accurate stellar abundance measurements. Indeed, the oxygen content in metal-poor stars is currently under debate (see Asplund & García Pérez 2001; Meléndez et al. 2001, 2006, and references therein).

Since the Sun is used as a fundamental reference in most areas of astrophysics, it is important to study all spectral features available for abundance analysis. Recent studies have mainly used the [O I] 6300, 6363 Å forbidden lines, the O I 7777 Å triplet, pure rotation OH lines as well as the fundamental vibration-rotation OH lines (Allende Prieto et al. 2001, 2004; Asplund et al. 2004), from which $\log \epsilon_{\text{O}} = 8.66 \pm 0.05$ have been recommended (Asplund et al. 2004). Meléndez (2004) presented a study of the first-overtone OH lines, which are unfortunately very weak for a precise determination of the oxygen abundance, but within the uncertainties these lines also support a low solar oxygen abundance.

Another independent way to estimate the solar oxygen abundance is using the forbidden line at 5577.34 Å. This line has been disregarded in the past due to blending with C_2 lines (e.g. Altrock 1968; Lambert 1978). Here, we present the first detailed study of the [O I] 5577 Å line, carefully taking into account the blends by C_2 lines. The advantage of this feature is that the C_2 blends introduce a large asymmetry in the profile, allowing thus to readily constrain their contribution. Another advantage is that there are other nearby C_2 lines that can be used to calibrate the blending C_2 lines, and therefore to determine a reliable solar oxygen abundance.

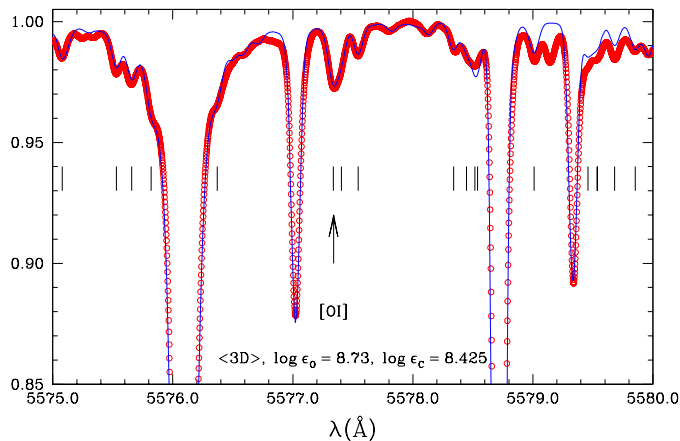


Fig. 1. Observed solar spectrum (Delbouille et al. 1973) between 5575 and 5580 Å (red circles) and the best fit employing the $\langle 3D \rangle$ model (solid blue line). The locations of the most prominent C_2 lines used to estimate the C abundance are denoted with vertical lines, while the position of the [O I] line is marked with an arrow. The resulting solar C abundance is $\log \epsilon_c = 8.42$ with which the 5577.3 Å feature implies a solar O abundance of $\log \epsilon_o = 8.73$.

2. Analysis

We used the Delbouille et al. (1973) disk-center solar spectrum (often called the Liege solar atlas), the Brault & Neckel (1987) disk-center intensity atlas (see Neckel 1999), and the Kurucz et al. (1984) solar-flux spectrum. These solar spectra are of extremely high resolution (resolving power $R \approx 500\,000 - 700\,000$) and have a S/N of several thousands at 5577 Å. The solar oxygen abundance obtained with these different atlases agree within $\sigma = 0.04$ dex. In Fig. 1 the Delbouille et al. (1973) solar spectrum around the 5577.3 Å [O I] line is shown as open circles.

The oscillator strength for the [O I] 5577 Å line is well determined: the mean of the available calculations is $\log gf = -8.25 \pm 0.03$ (Galavis et al. 1997; Baluja & Zeippen 1988; Fischer & Saha 1983; Nicolaides & Sinanoğlu 1973). We adopted $\log gf = -8.28$ from Galavis et al. (1997), which is on the same scale as the $\log gf$ value adopted for the 6300, 6363 Å forbidden lines (Asplund et al. 2004) within 0.007 dex; had we instead opted for the mean value of the above-mentioned theoretical gf -values our derived O abundance would be 0.03 dex lower. The excitation potential of the [O I] 5577 Å line is 1.967 eV. According to the NIST database¹ the observed and Ritz wavelengths are 5577.34 and 5577.339 Å, respectively. Small errors in the wavelength translate into only small uncertainties (at the level of 0.01 dex) in the O abundances.

We included in the spectral synthesis other atomic and molecular (C_2 Swan and CN red systems) lines present around 5577 Å, but the main contributors to the 5577.3 Å feature are mostly three lines: the [O I] line and the P_{127} and P_{226} lines of the C_2 (1-2) band. Atomic lines were taken from the latest Kurucz line lists² and the CN line list described in Meléndez & Barbuy (1999) was adopted. The line list for the 0-1 and 1-2 bands of the C_2 Swan system was constructed in a similar way to the 0-0 band described in Meléndez & Cohen (2007), but with the line positions taken primarily from Tanahashi et al. (2007)

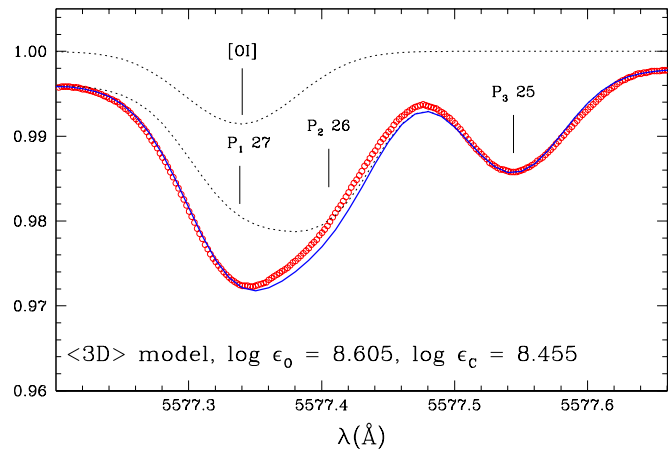
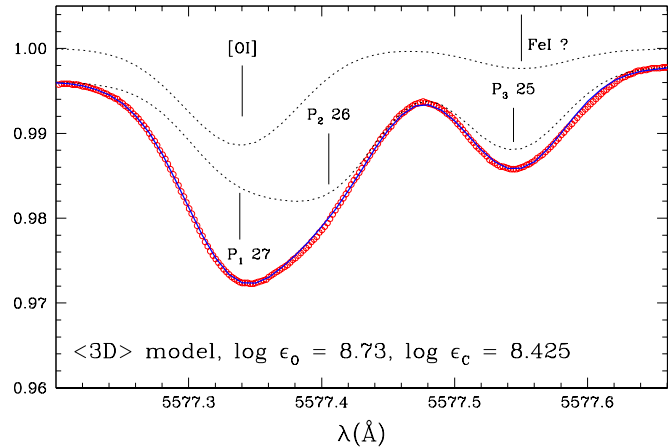


Fig. 2. *Upper panel:* An enlargement of the observed (red circles, Delbouille et al. 1973) and $\langle 3D \rangle$ -based theoretical profiles (solid blue line) shown in Fig. 1. The dotted lines show the separate contribution of [O I] and other lines labeled accordingly. The 5577.54 Å P_{325} C_2 line is blended with an unknown feature, assumed here to be Fe I. *Lower panel:* Same as above but assuming instead that the red feature is entirely due to P_{325} C_2 . Applying this 0.03 dex higher C abundance to the [O I]+ C_2 blend implies a smaller left-over contribution for [O I] and thus a 0.13 dex lower O abundance at the expense of a significantly poorer profile fit.

and complemented with Phillips & Davis (1968) for the higher excitation lines not included by Tanahashi et al.. Relative oscillator strengths for the 0-1 and 1-2 bands were taken from Kokkin et al. (2007), normalizing those values to the laboratory oscillator strength of the 0-0 band recommended by Grevesse et al. (1991), $f_{00} = 3.03 \times 10^{-2}$. The rotational strengths were computed following Kovacs (1961) and the rotational dependence of the band strengths was taken into account (Dwivedi et al. 1978).

A set of six different model atmospheres was employed: a three-dimensional hydrodynamical model of the solar atmosphere (Asplund et al. 2000; here denoted 3D) and its temporal and spatial average (here: $\langle 3D \rangle$) (Asplund et al. 2004), MARCS model (Asplund et al. 1997), Kurucz overshooting (Castelli et al. 1997) and the latest no-overshooting (Castelli & Kurucz 2004) models and the semi-empirical Howeger-Müller (1974) model. The spectral line formation was calculated in 3D and 1D using the same spectrum synthesis code as described in Asplund et al. (2004). The 1D calculations were also performed using the 2002 version of MOOG (Snedden 1973); the different 1D calculations with different codes agree at the level of 0.01 dex.

¹ <http://physics.nist.gov/PhysRefData/ASD/index.html>

² <http://kurucz.harvard.edu/>

The contribution from the two C_2 lines (P_{127} and P_{226}) to the 5577.3 Å feature can be well constrained from the red asymmetry in the profile. In addition there are many neighboring C_2 lines of very similar excitation potential and line strengths and thus basically identical line formation. Note that the error in the relative strengths of the C_2 lines is negligible, as the rotational strengths are precisely given by their Hönl-London factors (Kovacs 1961). Fig. 1 shows the best fit to the 5575-5580 Å region of the Liege disk-center atlas based on the 3D-averaged model atmosphere; the locations of the most important C_2 lines are marked with vertical lines. Clearly the overall agreement is quite satisfactory. Also encouraging is that the thus estimated solar C abundance is as expected for the different model atmospheres (Asplund et al. 2005). As seen in Fig. 2, the profile of the [O I]+ C_2 feature is very well described with this C abundance and a solar oxygen abundance of $\log \epsilon_O = 8.73^3$ with the <3D> model. The resulting disk-center intensity equivalent width for only the [O I] line is 1.23 mÅ, which corresponds to $\log \epsilon_O = 8.72$ for the full 3D model. The Kurucz et al. (1984) solar-flux and the Brault & Neckel (1987) intensity spectrum gave an O abundance 0.01 dex higher and -0.07 dex lower, respectively. Results for different model atmospheres are similar, as shown in Table 1, thus the [O I] 5577 Å line is almost insensitive to the adopted model atmosphere.

It should be noted that the predicted profile for the neighboring feature at 5577.55 Å is too weak with the C abundance from the overall fit to all C_2 lines in the wavelength window 5575-5580 Å (Fig. 2), suggesting that it is blended. Scouring available atomic databases did not reveal any likely candidates. We have therefore tentatively assigned the blending line as being due to Fe I but the exact choice is unimportant. Relying solely on the P_{325} transition and without accounting for this blend, the estimated C abundance would have been 0.03 dex higher. Because of the larger contribution from C_2 the [O I] part of the 5577.3 Å feature must decrease correspondingly, leading to a much reduced solar O abundance: $\log \epsilon_O \approx 8.6$. In this case, however, the profile fit is very unsatisfactory, in particular in the red wing, as evident in Fig. 2.

The main errors are the uncertainties in the $\log gf$ value of the [O I] line (assumed here to be 0.03 dex, which is the σ between the different calculations; c.f. Galavis et al. 1997; Baluja & Zeppen 1988; Fischer & Saha 1983; Nicolaides & Sinanoğlu 1973) and the observational error. Part of the observational error (0.04 dex) may be due to variation with solar activity (e.g. Livingston et al. 2007), and it was estimated by using different solar atlases. Note that Caffau et al. (2008) has also found a similar scatter (0.03 dex) between the [O I] 6300 Å oxygen abundances obtained from different solar atlases. The other part of the observational error (0.05 dex) was estimated by employing different assumptions with respect to the continuum determination and varying by 0.01 Å the wavelengths of the C_2 lines⁴ and of the unknown feature at 5577.55 Å. Given the excellent agreement between the oxygen abundance obtained from different model atmospheres for this spectral feature, we estimate that the er-

³ Note that the abundance quoted here is only from the Liege intensity atlas (Figs. 1 and 2). The final abundance given in Table 1 is based on the mean from the three different solar atlases.

⁴ According to Tanabashi et al. (2007) the line positions for those C_2 lines are not very precise, hence we allowed small changes by up to 0.01 Å in wavelength. Also, note that Allende Prieto & García López (1998) have shown that the Delbouille et al. solar disk-center intensity atlas have slight errors in its absolute wavelength calibration, although probably not over a wavelength scale of a few Å, which is relevant here.

rors introduced by problems in the model atmosphere should be 0.04 dex at most. Non-LTE effects for this [O I] line should be negligible (e.g. Altrrock 1968; Takeda 1994). Adding the squared errors (0.03 dex in the $\log gf$ value, 0.04 dex in the apparent line variation, 0.05 dex due to uncertainties in the continuum and line positions, and 0.04 dex in the models), we estimate a conservative total error of 0.08 dex.

3. Solar oxygen abundance from different diagnostics

Asplund et al. (2004) have determined the solar oxygen abundance from the [O I] 6300, 6363 Å forbidden lines, O I permitted lines, and the pure rotation and fundamental vibration-rotation OH lines, employing a 3D hydrodynamical simulation of the solar atmosphere as well as a 1D MARCS (Asplund et al. 1997) and the Holweger & Müller (1974) semi-empirical model atmospheres. Meléndez (2004) has added oxygen abundances determined from the first-overtone OH lines, as well as computed the solar oxygen abundance for the above features using the <3D> and Kurucz (Castelli et al. 1997) convective overshooting models. Here we add the 5577.3 Å forbidden line for the five model atmospheres described above, and we also have determined oxygen abundances for the latest Kurucz (Castelli & Kurucz 2004) model without convective overshooting.

The results of the different computations are summarized in Table 1, where the mean oxygen abundance for the forbidden lines now includes the 5577.3 Å line. The mean value given for the infrared OH lines includes all the OH mentioned above, but given half-weight to the pure rotation and the first-overtone line, because the pure rotation lines are quite sensitive to the detailed structure of the model atmosphere, while the first-overtone lines are very weak and the observational error is high. For the O I lines we adopt the mean non-LTE results of Allende Prieto et al. (2004) and Asplund et al. (2004), with and without including inelastic H collisions, respectively. As discussed by Asplund (2005), the H collisions are based on the classical but highly uncertain formula by Drawin (1968), yet the O abundance with (and without) collisions is only ≈ 0.03 higher (lower) than the mean O abundance adopted here. We also show in the last row the averaged solar oxygen abundance for each model atmosphere. In obtaining this mean value, half weight has been given to the result obtained from the molecular lines, because of their strong model atmosphere sensitivity.

As can be seen, all model atmospheres favor a low solar oxygen abundance: $\log \epsilon_O \approx 8.7$. The reduction in the solar oxygen abundance from the historical value of ≈ 8.9 (Anders & Grevesse 1989)⁵ to the present level is therefore not primarily driven by the use of a 3D hydrodynamic models. In this context, improvements in the input atomic and molecular data, more realistic non-LTE calculations and a more careful treatment of blends are equally important. The average O abundance for the 3D model presented here is 8.67, only 0.01 higher than the value recommended by Asplund et al. (2004, $\log \epsilon_O = 8.66 \pm 0.05$). Note that the recommended O abundance obtained with the Holweger & Müller (1974) model is only 0.04 dex higher than the 3D-based abundance but show the largest scatter (0.10 dex), mainly due to the large difference between OH and O I.

⁵ It should be noted that the solar O abundance of 8.83 given in the compilation of Grevesse & Sauval (1998) is only a preliminary analysis based on a Holweger-Müller (1974) model with a modified temperature structure to remove various abundance trends with excitation potential and line strengths for species such as Fe I, OH and CH.

Table 1. Solar oxygen abundance from different model atmospheres.

| lines | 3D | <3D> | Holweger-Müller | MARCS | Kurucz overshooting | Kurucz no overshooting |
|---------------------------|-------------|-------------|-----------------|-------------|---------------------|------------------------|
| [O I] 5577 Å ^a | 8.70±0.08 | 8.71 ± 0.08 | 8.73±0.08 | 8.70± 0.08 | 8.74 ± 0.08 | 8.70 ± 0.08 |
| [O I] | 8.69 ± 0.05 | 8.73 ± 0.05 | 8.75 ± 0.05 | 8.71 ± 0.05 | 8.77 ± 0.05 | 8.73 ± 0.05 |
| O I | 8.67 ± 0.05 | 8.68 ± 0.05 | 8.64 ± 0.08 | 8.72 ± 0.05 | 8.67 ± 0.05 | 8.64 ± 0.05 |
| OH | 8.61 ± 0.10 | 8.68 ± 0.10 | 8.85 ± 0.10 | 8.73 ± 0.11 | 8.80 ± 0.10 | 8.72 ± 0.10 |
| Average | 8.67 ± 0.04 | 8.70 ± 0.04 | 8.71 ± 0.10 | 8.72 ± 0.04 | 8.73 ± 0.07 | 8.69 ± 0.05 |

^a Average abundance from the Delbouille et al. (0.02 higher), Brault & Neckel (0.04 lower) and Kurucz et al. (0.03 higher) atlases.

Using $1/\sigma^2$ of the mean oxygen abundances given in Table 1 as weights (assuming a minimum $\sigma = 0.04$ dex) implies a weighted mean solar oxygen abundance from the six solar model atmospheres of $\log \epsilon_{\text{O}} = 8.70$ ($\sigma = 0.02$).

Higher solar O abundances have recently been advocated by Caffau et al. (2008) and Ayres (2008) based on the atomic lines and an alternative 3D solar model computed with the CO5BOLD code (Freytag et al. 2002); neither study includes the here employed [O I] 5577 Å line. Caffau et al. (2008) finds $\log \epsilon_{\text{O}} = 8.76$ with the main differences being the adopted equivalent widths and the less severe non-LTE abundance corrections for O I due to their inclusion of inelastic H collisions close to the Drawin (1968) recipe; it appears that the results of Asplund et al. (2004) and Caffau et al. (2008) in most cases are in excellent agreement when otherwise using the same line input data, in spite of some differences in the mean temperature stratification of the two 3D models. Ayres (2008) found $\log \epsilon_{\text{O}} = 8.81$ based on the [O I] 6300 Å line, which is blended by a Ni I line (Allende Prieto et al. 2001). In order to achieve the best overall profile fit, he had to use a solar Ni abundance lower by 0.15 dex than the value given by Grevesse et al. (2007). This is well outside the quoted uncertainties in the laboratory gf -value (Johansson et al. 2003) and the solar Ni abundance. Clearly more work is needed in order to resolve the existing issues with solar O abundance determinations using the different indicators. We are currently working towards this goal using a new, further improved 3D solar model with a more realistic radiative transfer treatment (e.g. opacity sampling instead of opacity binning).

4. Conclusions

A low oxygen abundance is obtained from the [O I] 5577.3 Å line, almost independent of the adopted model atmosphere: $\log \epsilon_{\text{O}} = 8.71 \pm 0.02 \pm 0.07$ (0.02 dex is the σ from using different models, and 0.07 dex is the error due to uncertainties in the the $\log gf$ value (0.03 dex), apparent line variation (0.04 dex) and uncertainties in the continuum and line positions (0.05 dex)). This value is close to the results of Asplund et al. (2004) and Meléndez (2004) for other solar oxygen abundance indicators (O I, [O I] and OH lines). Including those abundances and employing six different 3D and 1D model atmospheres, we estimate a solar O abundance of $\log \epsilon_{\text{O}} = 8.70$ ($\sigma = 0.02$) with only a small sensitivity to the employed model atmosphere.

The low solar oxygen abundance that we propose here as well as the downward revision of other solar chemical abundances (Asplund 2000, 2005, 2007; Asplund et al. 2000, 2005, 2006) pose a challenge to standard solar models in light of helioseismological observations (e.g. Antia & Basu 2005, 2006;

Bahcall et al. 2004, 2005, 2006; Basu & Antia 2004, 2008; Chaplin et al. 2007; Guzik et al. 2005; Yang & Bi 2007).

Acknowledgements. We thank A. Alves-Brito & B. Barbuy for sending a copy of the Phillips & Davis (1968) Berkeley atlas of the C₂ Swan system. This work has been supported by ARC (DP0588836) and FCT (project PTDC/CTE-AST/65971/2006).

References

- Allende Prieto, C., & Garcia Lopez, R. J. 1998, A&AS, 129, 41
Allende Prieto, C., Lambert, D. L., & Asplund, M. 2001, ApJ, 556, L63
Allende Prieto, C., Asplund, M., & Fabiani Bendicho, P. 2004, A&A, 423, 1109
Altrock, R. C. 1968, Sol. Phys., 5, 260
Anders, E., & Grevesse, N. 1989, Geochim. Cosmochim. Acta, 53, 197
Antia, H. M., & Basu, S. 2005, ApJ, 620, L129
Antia, H. M., & Basu, S. 2006, ApJ, 644, 1292
Asplund, M., Gustafsson, B., Kiselman, D., & Eriksson, K. 1997, A&A, 318, 521
Asplund, M. 2000, A&A, 359, 755
Asplund, M., Nordlund, Å., Trampedach, R., & Stein, R. F. 2000, A&A, 359, 743
Asplund, M., & García Pérez, A. E. 2001, A&A, 372, 601
Asplund, M., Grevesse, N., Sauval, A. J., Allende Prieto, C., & Kiselman, D. 2004, A&A, 417, 751
Asplund, M. 2005, ARA&A, 43, 481
Asplund, M., Grevesse, N., Sauval, A. J., Allende Prieto, C., & Blomme, R. 2005, A&A, 431, 693
Asplund, M., Grevesse, N., & Sauval, A. J. 2006, Communications in Asteroseismology, 147, 76
Asplund, M. 2007, IAU Symposium, 239, 122
Ayres, T. R., Plymate, C., & Keller, C. U. 2006, ApJS, 165, 618
Ayres, T. R. 2008, ApJS, submitted
Bahcall, J. N., Serenelli, A. M., & Pinsonneault, M. 2004, ApJ, 614, 464
Bahcall, J. N., Basu, S., & Serenelli, A. M. 2005, ApJ, 631, 1281
Bahcall, J. N., Serenelli, A. M., & Basu, S. 2006, ApJS, 165, 400
Baluja, K. L., & Zeippen, C. J. 1988, Journal of Physics B Atomic Molecular Physics, 21, 1455
Brault, J., & Neckel, H. 1987, Spectral atlas of solar absolute disk-averaged and disk-center intensity from 3290 to 12510 Å
Basu, S., & Antia, H. M. 2004, ApJ, 606, L85
Basu, S., & Antia, H. M. 2008, Phys. Rep., 457, 217
Caffau, E., Ludwig, H.-G., Steffen, M., Ayres, T. R., Bonifacio, P., Cayrel, R., Freytag, B., & Plez, B. 2008, A&A, in press (arXiv:0805.4398)
Castelli, F., Gratton, R. G., & Kurucz, R. L. 1997, A&A, 318, 841
Castelli, F., & Kurucz, R. L. 2004, A&A, 419, 725
Centeno, R., & Socas-Navarro, H. 2008, ApJ, in press (arXiv:0803.0990)
Chaplin, W. J., Serenelli, A. M., Basu, S., Elsworth, Y., New, R., & Verner, G. A. 2007, ApJ, 670, 872
Delbouille, L., Roland, G., & Neven, L. 1973, Liege: Universite de Liege, Institut d'Astrophysique, 1973
Drawin, H.-W. 1968, Zeitschrift fur Physik, 211, 404
Dwivedi, P. H., Branch, D., Huffaker, J. N., & Bell, R. A. 1978, ApJS, 36, 573
Fischer, C. F., & Saha, H. P. 1983, Phys. Rev. A, 28, 3169
Freytag, B., Steffen, M., & Dorch, B. 2002, Astronomische Nachrichten, 323, 213
Galavis, M. E., Mendoza, C., & Zeippen, C. J. 1997, A&AS, 123, 159
Grevesse, N., Sauval, A. J., & van Dishoeck, E. F. 1984, A&A, 141, 10

- Grevesse, N., Lambert, D. L., Sauval, A. J., van Dishoek, E. F., Farmer, C. B., & Norton, R. H. 1991, *A&A*, 242, 488
- Grevesse, N., & Sauval, A. J. 1998, *Space Science Reviews*, 85, 161
- Grevesse, N., Asplund, M., & Sauval, A. J. 2007, *Space Science Reviews*, 130, 105
- Guzik, J. A., Watson, L. S., & Cox, A. N. 2005, *ApJ*, 627, 1049
- Holweger, H., & Müller, E. A. 1974, *Sol. Phys.*, 39, 19
- Holweger, H. 2001, Joint SOHO/ACE workshop "Solar and Galactic Composition", 598, 23
- Johansson, S., Litzén, U., Lundberg, H., & Zhang, Z. 2003, *ApJ*, 584, L107
- Kokkin, D. L., Bacskay, G. B., & Schmidt, T. W. 2007, *J. Chem. Phys.*, 126, 4302
- Kovacs, I. 1961, *Rotational structure in the spectra of Diatomic Molecules* (London: Hilger)
- Kurucz, R. L., Furenlid, I., Brault, J., & Testerman, L. 1984, *National Solar Observatory Atlas, Sunspot*, New Mexico: National Solar Observatory, 1984,
- Lambert, D. L. 1978, *MNRAS*, 182, 249
- Livingston, W., Wallace, L., White, O. R., & Giampapa, M. S. 2007, *ApJ*, 657, 1137
- Meléndez, J., & Barbuy, B. 1999, *ApJS*, 124, 527
- Meléndez, J., Barbuy, B., & Spite, F. 2001, *ApJ*, 556, 858
- Meléndez, J. 2004, *ApJ*, 615, 1042
- Meléndez, J., Shchukina, N. G., Vasiljeva, I. E., & Ramírez, I. 2006, *ApJ*, 642, 1082
- Meléndez, J., & Cohen, J. G. 2007, *ApJ*, 659, L25
- Neckel, H. 1999, *Sol. Phys.*, 184, 421
- Nicolaides, C. A., & Sinanoğlu, O. 1973, *Sol. Phys.*, 29, 17
- Phillips, J. G., & Davis, S. P. 1968, *Berkeley Analyses of Molecular Spectra*, Berkeley: University of California Press, 1968,
- Sauval, A. J., Grevesse, N., Zander, R., Brault, J. W., & Stokes, G. M. 1984, *ApJ*, 282, 330
- Snedden, C. A. 1973, PhD thesis, AA(THE UNIVERSITY OF TEXAS AT AUSTIN.)
- Socas-Navarro, H., & Norton, A. A. 2007, *ApJ*, 660, L153
- Takeda, Y. 1994, *PASJ*, 46, 53
- Tanabashi, A., Hirao, T., Amano, T., & Bernath, P. F. 2007, *ApJS*, 169, 472
- Yang, W. M., & Bi, S. L. 2007, *ApJ*, 658, L67